

A Novel High Throughput Biochemical Assay to Evaluate the HuR Protein-RNA Complex Formation

Vito G. D'Agostino¹, Valentina Adami², Alessandro Provenzani^{1*}

1 Laboratory of Genomic Screening, Centre for Integrative Biology, University of Trento, Mattarello, Trento, Italy, **2** High Throughput Screening core facility, Centre for Integrative Biology, University of Trento, Mattarello, Trento, Italy

Abstract

The RNA binding protein HuR/ELAVL1 binds to AU-rich elements (AREs) promoting the stabilization and translation of a number of mRNAs into the cytoplasm, dictating their fate. We applied the AlphaScreen technology using purified human HuR protein, expressed in a mammalian cell-based system, to characterize *in vitro* its binding performance towards a ssRNA probe whose sequence corresponds to the one present in TNF α 3' untranslated region. We optimized the method to titrate ligands and analyzed the kinetic in saturation binding and time course experiments, including competition assays. The method revealed to be a successful tool for determination of HuR binding kinetic parameters in the nanomolar range, with calculated K_d of 2.5 ± 0.60 nM, k_{on} of $2.76\pm 0.56\cdot 10^6$ M⁻¹ min⁻¹, and k_{off} of 0.007 ± 0.005 min⁻¹. We also tested the HuR-RNA complex formation by fluorescent probe-based RNA-EMSA. Moreover, in a 384-well plate format we obtained a Z-factor of 0.84 and an averaged coefficient of variation between controls of 8%, indicating that this biochemical assay fulfills criteria of robustness for a targeted screening approach. After a screening with 2000 small molecules and secondary verification with RNA-EMSA we identified mitoxantrone as an interfering compound with rHuR and TNF α probe complex formation. Notably, this tool has a large versatility and could be applied to other RNA Binding Proteins recognizing different RNA, DNA, or protein species. In addition, it opens new perspectives in the identification of small-molecule modulators of RNA binding proteins activity.

Citation: D'Agostino VG, Adami V, Provenzani A (2013) A Novel High Throughput Biochemical Assay to Evaluate the HuR Protein-RNA Complex Formation. PLoS ONE 8(8): e72426. doi:10.1371/journal.pone.0072426

Editor: Albert Jeltsch, Universität Stuttgart, Germany

Received: April 18, 2013; **Accepted:** July 10, 2013; **Published:** August 12, 2013

Copyright: © 2013 D'Agostino et al. This is an open-access article distributed under the terms of the Creative Commons Attribution License, which permits unrestricted use, distribution, and reproduction in any medium, provided the original author and source are credited.

Funding: This project has been carried out by using University of Trento, CIBIO start-up funds. The funders had no role in study design, data collection and analysis, decision to publish, or preparation of the manuscript.

Competing interests: The authors have declared that no competing interests exist.

* E-mail: provenzani@science.unitn.it

Introduction

The stability of a specific mRNA is dependent upon both cis-elements and trans-acting factors such as RNA binding proteins (RBPs). HuR/ELAVL1, initially discovered to be essential for the development of the *Drosophila melanogaster* nervous system [1], is a widely studied RBP that binds preferentially to AU-rich elements (AREs) mainly localized in the 3' untranslated region (UTR) of mRNAs [2,3], although other consensus binding elements have emerged [4], mainly with a stabilizing effect in the target mRNA. HuR shares with closely related RBPs of the Embryonic Lethal Abnormal Vision (ELAV) protein family a common characteristic structure of three highly conserved RNA recognition motifs (RRMs), of which the two tandem N-terminal RRM domains confer high affinity for ARE sequences [5,6]. The functional relevance of HuR-driven post-transcriptional regulation is pivotal in many pathologies, wherein occurrence and progression tightly correlate with a dysregulation in mRNA stability, including chronic inflammation, cardiovascular diseases, cancer, and

also resistance to chemotherapy [7–11]. High turnover mRNAs that form complexes with HuR (see review [7]) are usually studied by ribonucleo-immunoprecipitation coupled to immunoblotting/RT-PCR or by RNA-Electrophoresis Mobility Shift Assays (REMSAs). However, these approaches have several limitations due to the necessity of good antibodies for immunoprecipitation and to the assumption that complexes observed in non-denaturing gels are a good approximation of the cellular events. We therefore decided to develop a biochemical tool, based on AlphaScreen technology, that could complement traditional biochemical methods in the rapid and sensitive evaluation of HuR-RNA interaction and of competition with other trans-acting factors (direct or indirect protein-protein interactions). To this aim, we exploited the affinity between HuR and the AU-rich region of the TNF α 3' UTR mRNA for the development of our tool. Indeed, several reports have described the stabilization function and translational impact of HuR towards the TNF α mRNA [12–15]. Here we show that full-length human HuR protein can be functionally expressed in mammalian cells and the binding kinetic parameters,

at different time points by mixing equal volumes of complex 1 and complex 2 and the signals of the whole 384-well plate were detected at the end of the time course. The kinetics was performed in duplicate with two different protein preparations. Association and dissociation rate constants were determined from nonlinear regression fits of the data according to association kinetic model of multiple ligand concentration in GraphPad Prism®, version 5.0. The resulting K_d values obtained by k_{off}/k_{on} ratio were compared with the K_d of saturation binding experiments.

Competitive assays

Unlabeled RNA oligos (U-TNF) were mixed, at different concentration, with Bi-TNF probe (50 nM). These substrates were reacted with 1 nM of rHuR in the experimental condition of saturation binding and the signals were acquired when the reaction reached equilibrium (60 min later). Protein competition assays were carried out by performing rHuR-Bi-TNF binding reaction, with Acceptor and Donor beads, for 15 min and then different nanomolar rTTP and BSA concentrations were added. Nonspecific binding was subtracted and percentage of inhibition were plotted for the assays. The equilibrium dissociation constants (K_i) of U-TNF and rTTP ligands were determined from nonlinear regression fits of the data according to 1-site fit K_i model in GraphPad Prism®, version 5.0, by keeping constant the concentration (50 nM) and the K_d (2.5 nM) of the labeled Bi-TNF probe and by assuming that the binding was reversible and at equilibrium.

RNA-Electrophoresis Mobility Shift Assay (REMSA)

rHuR and Cy-TNF RNA probe were reacted in low micromolar concentration, as indicated, in buffer E (20 mM HEPES pH 7.5, 50 mM KCl, 0.5 μ g BSA, 0.25% Glycerol) in a final volume of 20 μ l at room temperature. For supershift experiments 0.5 μ g of anti-HuR antibody was added 10 min after preincubation of ligands. The reaction mix was then loaded onto 6% native polyacrylamide gel containing 0.5% Glycerol. Run was performed in 0.5X TBE buffer at 45 V and 4°C for 3 hr. Free and complexed RNA probe were detected with Typhoon Instrument (GE Healthcare; 00-4277-85 AC) using filters for red light emission detection.

High Throughput Screening of small molecules

AlphaScreen assay was optimized in a final volume of 20 μ l, with 1 nM of rHuR, 50 nM of RNA probe, and 20 μ g/ml of beads. Experiments for assay quality and robustness evaluation were initially performed using two 384-Optiplates with random distribution of Bi-TNF positive and Bi-TNFneg negative controls. In the primary screening of the small molecules, controls (Bi-TNF positive, Bi-TNFneg negative, DMSO) were located in the first and in the last two columns of the 384-Optiplates and each compound was tested in duplicate, in single dose and in different plates. Molecules were tested at the final concentration of 25 nM and all the dispensation steps were performed by the 96 channels pipetting head of a Tecan EVO 200 (Tecan, Switzerland). Primary screen was performed with a 2000 molecules library (Spectrum Collection, MicroSource Discovery, USA),

containing 60% of clinically used drugs, 25% of natural products and 15% of other bioactive components. Data and statistics were analyzed by GraphPad Prism®, version 5.0, software. Z-factor value was calculated with the equation: $1 - [3(SD_p + SD_n) / (M_p - M_n)]$, while Z-score values were calculated as: $(X - M_p) / SD_p$, where SD is the standard deviation, M is the mean, (p) and (n) are positive and negative controls, respectively, and X indicates fluorescence intensity of compound [18]. Competitive REMSA were performed as described above but using 0.5 μ M of compound, 0.2 μ M of rHuR protein and 0.5 μ M Bi-TNF probe.

Results

Purification and functional binding of recombinant HuR proteins

We produced human recombinant HuR (rHuR) protein from HEK293T cells. By transient transfection of HEK293T cells with pTrueORF-HuR plasmid we purified rHuR protein with both c-Myc and His6X tag in the C-terminal region. rHuR showed high purity after four steps of imidazole elution and western blot analysis confirmed a single band of the expected size (~38 kDa) (Figure 1A). The average protein yield, per 10 cm-dish with 80% confluent cells at the moment of transfection, was 1.5 μ g. In order to characterize the binding activity of rHuR to the TNF α ARE consensus we applied AlphaScreen technology using a 5'-biotinylated ssRNA sequence as substrate [15] (Bi-TNF). We optimized the assay to identify the best molar ratio between the two interacting partners coupled with anti-c-Myc-Acceptor and Streptavidin-Donor beads (Figure 1B); the optimal concentration was 1 nM and 50 nM for rHuR and Bi-TNF, respectively. The "hooking effect", where high concentrations of analyte exceed the binding capacity of the beads and lead to a reduced signal, was determined by single titrations showed in Figure 1C. We identified the formation of rHuR-RNA probe complex using nondenaturing and non cross-linked REMSA (Figure 2A) after mixing equimolar amount (0.5 μ M) of protein and Cy3-tagged TNF probe (Cy-TNF). As shown in the mobility shift assay, rHuR clearly caused the RNA probe electrophoretic retardation detectable as one prominent band, and the addition of the anti-HuR antibody in the binding reaction was able to produce the typical supershift of the RNA-protein complex. In these steps, we produced and purified the human recombinant HuR protein from HEK293T cells in its active form able to bind to ARE probes in two different biochemical assays. In comparison, optimal protein concentration for AlphaScreen assays resulted in 500 times lower than the amount required for a standard REMSA.

Characterization of rHuR binding to Bi-TNF probe

In accordance with AlphaScreen optimization data, rHuR binding kinetic was dependent on the concentration of the labeled Bi-TNF oligonucleotide and specific binding was consistent with the presence of AU-rich sequences in the substrate. Saturation binding experiments (Figure 2B) showed that rHuR has high affinity for Bi-TNF, with K_d value of 2.5 ± 0.60 nM, which is in line with K_d values of other reports characterizing human HuR protein expressed in *E. coli* cells

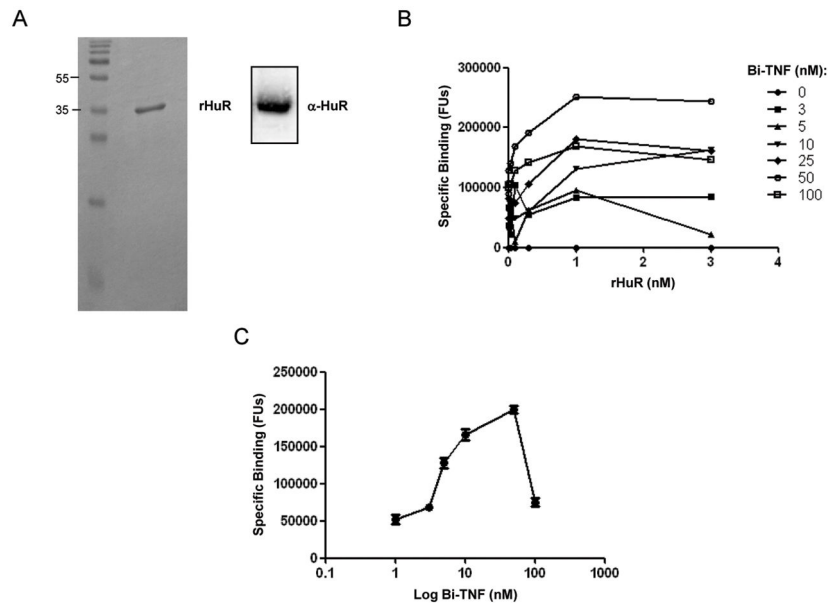


Figure 1. Purification of rHuR and optimization of the AlphaScreen assay. **A)** Representative 15% SDS-PAGE and Coomassie staining of purified rHuR protein (80 ng) recovered after Zeba™ Spin Desalting Columns dialyzed and western blot on the same sample (20 ng) using a polyclonal anti-HuR antibody. **B)** Bi-TNF RNA probe and rHuR protein double titration to determine optimal ligand concentrations with the AlphaScreen anti-c-Myc-Acceptor and streptavidin-Donor beads of the c-Myc detection kit (PerkinElmer), resulting in 1 nM and 50 nM for rHuR and Bi-TNF, respectively. **C)** Bi-TNF titration with 1 nM of rHuR. “Hooking effect” is shown for concentrations over 50 nM of RNA ligand (as the point at 100 nM in the log scale). Mean and standard deviation values derive from four independent experiments with four rHuR protein preparations.

doi: 10.1371/journal.pone.0072426.g001

[19,20]. As expected, absence of the Uridine tandem in the Bi-TNFneg probe caused the loss of ligand interactions, as shown by the fluorescence signal near to background, making this RNA probe an ideal negative control. Time course experiments showed that binding of rHuR to Bi-TNF probe was both time and dose dependent (Figure 2C). Data were globally fitted using the association kinetic model of multiple ligand concentration: derived association (k_{on} of $2.76 \pm 0.56 \times 10^6 \text{ M}^{-1} \text{ min}^{-1}$) and dissociation (k_{off} of $0.007 \pm 0.005 \text{ min}^{-1}$) rates indicated a very high affinity of the rHuR protein towards this RNA substrate and a low dissociation probability, as also reported by Kim et al 2011. According to the law of mass action, the equilibrium binding constant Kd calculated as k_{off}/k_{on} was absolutely indistinguishable from Kd values obtained by saturation experiments, indicating that the thermodynamic equilibrium was reached after 20 min of incubation. To assess if AU rich elements derived from different 3' UTR than TNF α showed similar properties, we chose to examine the binding affinity towards a ssRNA derived from the ARE of the COX-2 3' UTR [20]. In saturation binding experiments the Kd was $4.583 \pm 1.2 \text{ nM}$, indicating that this assay has a broad potential to investigate many different mRNA targets (Figure S1).

Utilization in competition experiments

In order to determine if this assay could be applied to evaluate competitive interactions we challenged the complex formation reaction by using untagged TNF α RNA probe (U-

TNF). U-TNF was added to the reaction keeping constant the concentration of Bi-TNF (50 nM) and replicating the experimental condition of saturation binding. U-TNF would interfere with the thermodynamic equilibrium of the complex formation if a decrease of the signal intensity proportional to U-TNF amount is observed. Indeed, U-TNF nicely titrated the complex (k_i of $4.49 \pm 1.1 \text{ nM}$) substituting Bi-TNF and increasing the percentage of inhibition in a dose dependent manner (Figure 3A). Furthermore, we expressed the recombinant His-Strep-tagged TTP protein (rTTP) in HEK293T cells through strep-tactin resin purification (Figure 3B). TTP competes with HuR intracellularly for binding to TNF α mRNA and this interplay dictates the translational efficiency of the target mRNA: HuR favors the polysomal recruitment of TNF α mRNA and facilitates its translation; in contrast, signaling cascades that activate TTP are responsible for the competition of this RBP against the same substrate leading to translational stop and/or RNA degradation [11,16]. We tested by REMSA the binding capability of purified rTTP by reacting a small amount of protein, as indicated, with $0.5 \mu\text{M}$ of Bi-TNF (Figure 3C). In the gel, multiple protein-RNA probe complexes were observed, as also previously reported for TTP protein [21,22], demonstrating that rTTP was active and highly sensitive to this substrate. Competition AlphaScreen assays as function of rTTP concentration (0–3 nM) showed the direct interaction of rHuR and rTTP proteins towards the same Bi-TNF probe (Figure 3D). According to our data, equilibrium dissociation constant k_i of

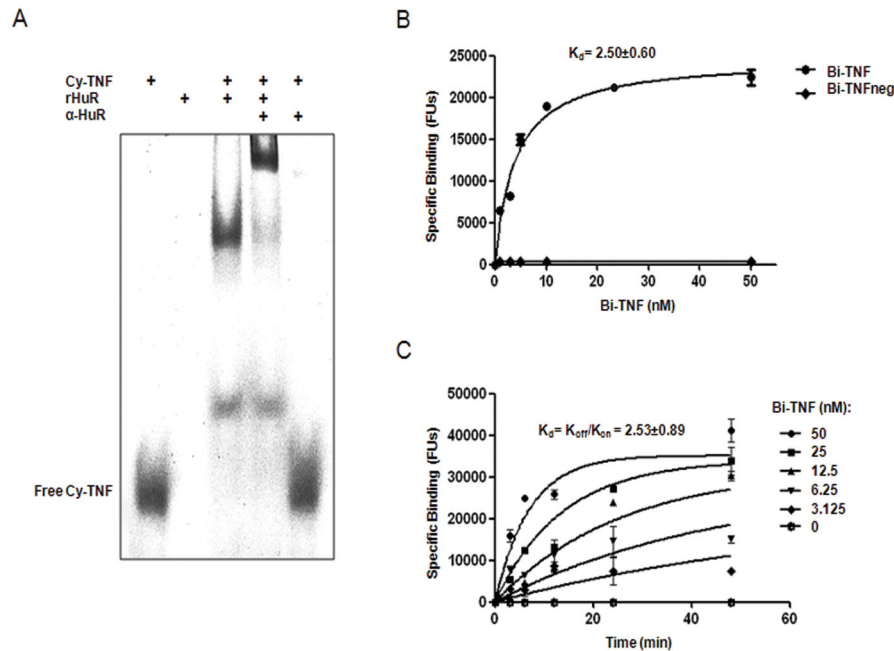


Figure 2. Characterization of the functional binding of rHuR to the AU-rich RNA substrate. **A)** REMSA showing the binding capability of rHuR (0.5 μ M) resulting in the presence of an higher molecular weight protein-RNA complex with respect to the free Cy-TNF RNA probe (0.5 μ M). The supershift caused by the anti-HuR antibody (1 μ g) indicates the presence of at least a ternary complex and the qualitative binding of rHuR. **B)** Saturation binding experiments. Equilibrium dissociation constants (K_d) were determined from nonlinear regression fits of the data according to a 1-site binding model in GraphPad Prism®, version 5.0. Mean and standard deviation values derive from four independent experiments with four rHuR protein preparations. **C)** Time course experiments. Association (K_{on}) and dissociation (K_{off}) rate constants were determined from nonlinear regression fits of the data according to association kinetic model of multiple ligand concentration in GraphPad Prism®, version 5.0. Mean and standard deviation values derive from two independent experiments with two rHuR protein preparations.

doi: 10.1371/journal.pone.0072426.g002

the competitive displacement was $1.76 \pm 0.41 \times 10^{-3}$ nM, suggesting that rTTP has higher affinity than rHuR towards the ARE substrate and approximately ten-fold molar excess of rHuR seems necessary to initiate competition for displacement of rTTP. In this context, appropriate AlphaScreen assay should be designed to precisely measure rTTP binding kinetics and association/dissociation rate constants. To investigate how post-translational modifications, such as phosphorylations, could impact on the binding affinity of rHuR we stimulated transfected cells for 3 hr with cyclosporine (CsA) [4 μ M], a compound able to induce in 786-0 renal cancer cells the HuR nucleo-cytoplasmic shuttling, its association with PKC- δ and its phosphorylation [23]. The CsA treatment in HEK293T cells did not affect the total amount of rHuR production in comparison with rHuR purified from control (DMSO) cells (Figure 3E) and it clearly induced an heavy phosphorylation pattern on the recombinant protein (P-rHuR), detectable using an anti-phosphoserine antibody. Saturation binding experiments (Figure 3F) revealed a not statistically significant K_d for P-rHuR (3.1 ± 0.55 nM, P value = 0.59) and a not statistically significant association kinetics (data not shown), indicating that the phosphorylations induced by CsA do not modify the binding properties of the protein in this *in vitro* assay.

AlphaScreen High Throughput Screening

As we added the same amount of rTTP and BSA after 20 min of rHuR-Bi-TNF incubation and the signals were detected 60 min later, we have thought that if rTTP had interfered with the thermodynamic equilibrium of the reaction we could exploit the AlphaScreen assay in a biochemical screening to identify molecules potentially targeting and inhibiting HuR-RNA interaction. In 384-well plate format we performed binding reaction with Bi-TNF positive and Bi-TNFneg negative controls. Coefficient of variations (CV) less than 15% and, importantly, a Z-factor value of 0.84 with a signal to background ratio (S/B) of 42 indicated that the assay was robust and reliable (Figure 4A). As a pilot screening experiment, we tested a library of 2000 small molecules, at the final concentration of 25 nM, looking for candidate molecule able to inhibit the rHuR-Bi-TNF complex formation. Effectively, as shown in Figure 4B, taking into account the induced auto-fluorescence of each compound and correction for unspecific binding, we ranked the library compounds according to their ability to affect the protein-RNA interaction (Full list is available in Table S1, Table S2). From the primary screening it has not been possible to discern between interfering compounds and real inhibitors of complex formation. Indeed interfering phenomena could be ascribed to

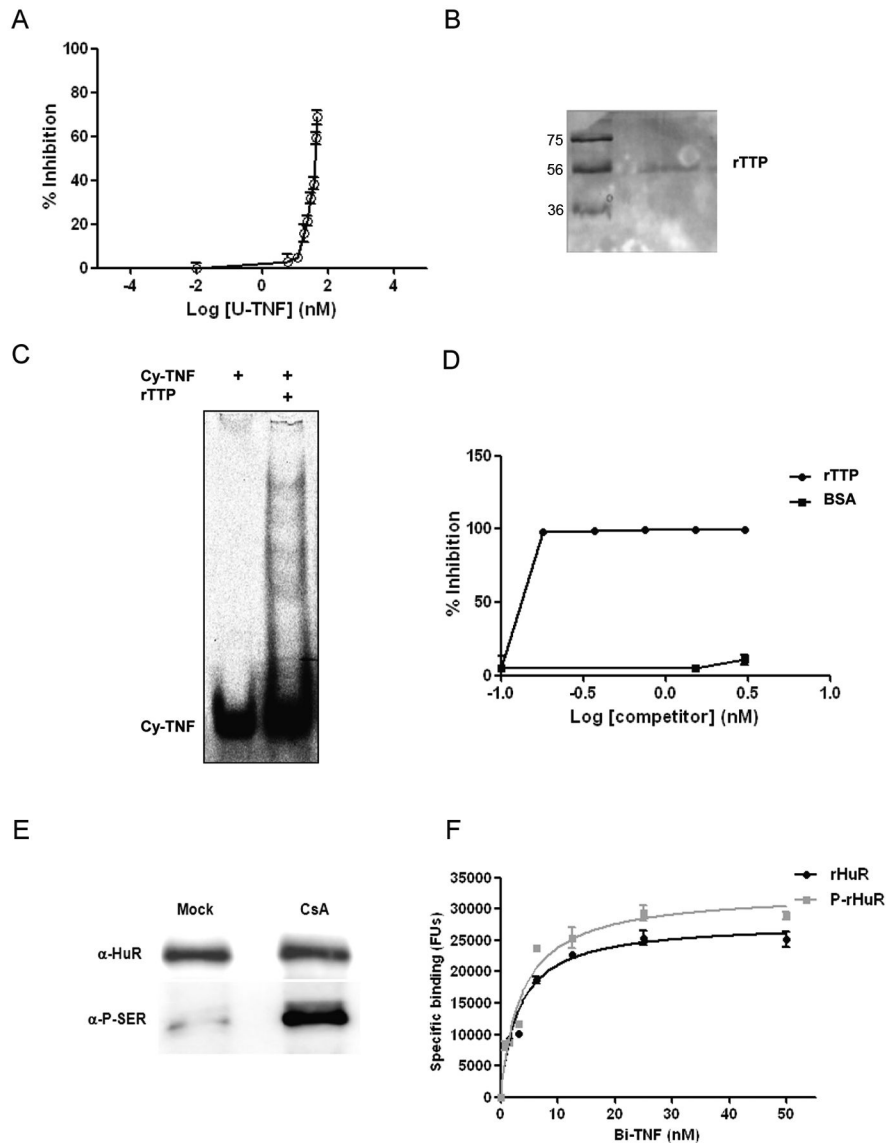


Figure 3. Competition assays with unmarked RNA oligonucleotide and with rTTP protein. **A**) The percentage of inhibition increased as function of untagged TNF α RNA probe (U-TNF) concentration. U-TNF was added to the reaction together with Bi-TNF probe and signals were detected at equilibrium. K_i values were determined from nonlinear regression fits of the data according to 1-site fit K_i model in GraphPad Prism®, version 5.0, by keeping constant the concentration (50 nM) and the K_d (2.5 nM) for the labeled Bi-TNF probe. Mean and standard deviation values derive from two independent experiments. **B**) Coomassie staining of purified and recovered Zeba™ Spin desalted rTTP protein (25 ng) loaded on 15% SDS-PAGE. **C**) REMSA showing rTTP (0.1 μ M) complexed with Cy-TNF RNA probe (0.5 μ M reacted and loaded on native gel). **D**) Competitive AlphaScreen assay as a function of rTTP concentration. Equal amounts of BSA were independently reacted as negative control. K_i values were determined from nonlinear regression fits of the data according to 1-site fit K_i model in GraphPad Prism®, version 5.0, by keeping constant the concentration (50 nM) and the K_d (2.5 nM) for the labeled Bi-TNF probe. Mean and standard deviation values derive from two independent experiments with two rTTP protein preparations. **E**) Western blot showing rHuR purified from control (Mock; DMSO) and CsA [4 μ M] stimulated HEK293T cells. After 3 hr of treatment the total amount of purified rHuR proteins (150 ng loaded on gel) was not affected, while the phosphorylation of the protein was clearly induced, as showed by an anti-phosphoserine antibody (P-SER). **F**) Saturation binding experiments comparing the binding capability of rHuR and phosphorylated rHuR (P-rHuR). Nonlinear regression fits of the data revealed an equilibrium dissociation constants equal to 3.1 ± 0.55 nM for P-rHuR, not statistically relevant (P value = 0.59) with respect to the K_d of rHuR. Mean and standard deviation values derive from two independent experiments.

doi: 10.1371/journal.pone.0072426.g003

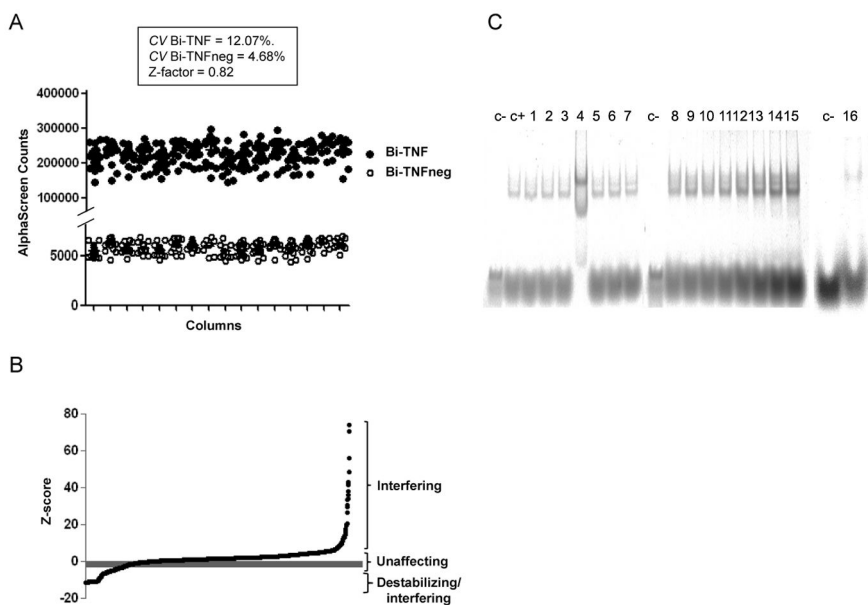


Figure 4. Robustness of the miniaturized AlphaScreen assay and screening of a drug library. **A)** rHuR and Bi-TNF positive or Bi-TNFneg negative controls were reacted at optimized nanomolar concentrations in a final volume of 20 μ l in 384-wells Optiplates. Relative coefficient of variations and Z-factor value are reported. **B)** Plot of progressive Z-score values of 2000 compounds according to their interference to rHuR-RNA complex formation assay. **C)** Representative REMSA showing the effect of compounds, selected after counter screening assay, on rHuR-RNA complex formation. Lane 1: Bi-TNF probe only; Lane 2: rHuR-Bi-TNF; Lane 3-9: 1-Aspartame, 2-Cephadrine, 3-Clomiphene citrate, 4-Cetylpyridinium chloride, 5-Diloxanide furoate, 6-Gentian violet, 7-Hydroquinone; Lane 10: Bi-TNF probe only; Lane 11-18: 8-Tilmicosin, 9-Nonoxynol-9, 10-Orlistat, 11-Protoveratrine, 12-Raloxifene hydrochloride, 13-Salsalate, 14-Switenolide diacetate, 15-Tetrandrine; Lane 19: Bi-TNF probe only; Lane 20: 16-Mitoxantrone hydrochloride. Compounds (0.5 μ M) were added to a binding reaction containing, as in Line 2, 0.2 μ M rHuR and 0.5 μ M Bi-TNF.

doi: 10.1371/journal.pone.0072426.g004

technical artifacts, such as beads-molecule cross-talk or photochemical singlet oxygen generation/quenching, nevertheless to specific influence on RNA/rHuR conformational status. For these reason, 10% of hits classified as destabilizers in the primary screening were re-screened and the first 16 further tested by REMSA as secondary assay (Figure 4C). Cethylpyridinium choride (lane 6) and Mitoxantrone (lane 16) clearly influenced the formation of the protein-RNA complex demonstrating the validity of the approach used and suggesting this method can be used in screening with wider chemical libraries.

Discussion

We have recently applied the AlphaScreen technology to quantitatively discriminate the affinity of HuR towards RNA probes carrying ARE consensus sequences by comparing the binding to TNF α and p62 mRNA probes [24]. Here we finely dissect the potentiality of this assay measuring the binding kinetic properties, including association and dissociation rate constants, that regulate the binding of the full-length human recombinant HuR protein expressed in mammalian cells to the TNF α ARE-bearing mRNA probes. REMSA has been the tool of choice to investigate the binding capability of HuR towards

target mRNAs since the first reported experiments [15]. However, although gel electrophoresis can give useful information about the molecular species present in the complex formation, REMSAs are cumbersome experiments, quantitative and qualitative amenable only for low throughput drug testing [25]. We focused our work to the development of a sensitive assay that could quantify the formation of the rHuR-RNA complex and that could be used in high throughput drug screening experiments. In this context, a previous approach has made use of recombinant truncated HuR protein and fluorescence intensity distribution analysis (FIDA) to specifically identify low-molecular-weight HuR inhibitors. By a mathematical model that could fit experimental evidences it has been shown HuR homodimerization before binding to RNA probe, with a stoichiometry of 2:1, protein: RNA respectively [20,26]. The strategy used in our assay allows to identify molecules that can interfere with complex formation, since the different competition of both U-TNF and rTTP specifically brought to a decrease on the ligands interactions. From saturation binding experiments we calculated a K_d , indistinguishable from the dissociation constant value of the k_{off}/k_{on} ratio, quantified in the nanomolar range, indicating the sensitivity of the assay and the high affinity of the protein towards this RNA substrate. This addresses HuR-mRNA TNF α

complex formation as a tightly controlled interaction as often highlighted in many reports [27–29]. Of note, observed association rate constants (data not shown) in time course experiments were linearly proportional to RNA probe concentration, describing a pseudo-first order association kinetic. However, precise determination of stoichiometric relationships between ligands is difficult here because estimation of Acceptor and Donor beads binding capacities and additional dissociation kinetic experiments are needed. Although we could not discriminate between the binding affinity of rHuR and P-rHuR to Bi-TNF we cannot exclude that further refinements of the assay such as site specific modifications of the post-translational pattern of the protein or a different design of the mRNA probe, would result in a differential binding affinity associated with post-translational modifications. Finally we report here the results of a 2000 molecules screening and the identification of a number of compounds that interfere with the assay or with rHuR-Bi-TNF complex formation. In the context of HTS applications, utilization of beads-based assays and, more importantly, of a readout that is strongly dependent on the redox species present in the binding buffer suggests particular care in the biological interpretation of data and, consequently, in their functional aspects. Consequently, hits are expected to be further characterized for mechanistic, pharmacological and biological relevance. Among the hits, Mitoxantrone revealed to be a compound interfering with rHuR binding to Bi-TNF in both of our *in vitro* assays. Since the anthracenedione scaffold was reported in previous screening for HuR inhibitors [26], we can consider the presence of this drug among our hits as a *bona fide* control of the robustness of our approach. This drug has been used for many years as an antitumoral agent [30], is a known ligand of nucleic acid [31] and it has been re-addressed for utilization in multiple sclerosis [32]. The inhibitory effect on complex formation we report here could be due to its unspecific property to precipitate mRNA [33], however mitoxantrone has been reported as a stabilizer of the tau pre-mRNA stem loop [34] after a screening of about 110000 molecules, suggesting the mRNA binding property of this molecule may relate to its pharmacology. Therefore it may also suggest that its inhibition activity of TNF α secretion [31] or its anticancer activity can partially depend on the interference with HuR-TNF α complex formation *in vivo*. Further studies are needed to elucidate this

point. In summary, we have developed and characterized a quantitative and straightforward biochemical assay amenable for high throughput screening platforms. As a new tool it can open new perspectives in the elucidation of HuR binding ability in solution and may pave the way towards the identification of low-molecular-weight inhibitors specifically designed to break HuR-targeted mRNA interaction.

Supporting Information

Figure S1. Characterization of the functional binding of rHuR to the AU-Rich Element of TNF α and COX-2 3' UTRs.

By saturation binding experiment, equilibrium dissociation constants (Kd) were determined from nonlinear regression fit of the data according to a 1-site binding model in GraphPad Prism®, version 5.0. Kd to Bi-COX is reported with standard error, Kd to Bi-TNF confirmed to be 2.751 nM. (TIF)

Table S1. List of 2000 molecules evaluated in the primary screening with corresponding Z-score.

(XLS)

Table S2. List of 218 molecules evaluated in the secondary screening with corresponding Z-score.

Molecules evaluated in REMSAs are the first 16 of the secondary screening.

(XLS)

Acknowledgements

We are grateful to prof. Gaestel and dr Tiedje for kindly providing the plasmids for TTP expression.

Author Contributions

Conceived and designed the experiments: VGD AP. Performed the experiments: VGD VA. Analyzed the data: VGD VA AP. Contributed reagents/materials/analysis tools: VGD VA AP. Wrote the manuscript: VGD AP.

References

- Burd CG, Dreyfuss G (1994) RNA binding specificity of hnRNP A1: significance of hnRNP A1 high-affinity binding sites in pre-mRNA splicing. *EMBO J* 5: 1197-1204. PubMed: 7510636.
- Chen CY, Shyu AB (1995) AU-rich elements: characterization and importance in mRNA degradation. *Trends Biochem Sci* 11: 465-470. PubMed: 8578590.
- Fan XC, Steitz JA (1998) HNS, a nuclear-cytoplasmic shuttling sequence in HuR. *Proc Natl Acad Sci U S A* 26: 15293-15298.
- Dassi E, Zuccotti P, Leo S, Provenzani A, Assfalg M et al. (2013) Hyper conserved elements in vertebrate mRNA 3'-UTRs reveal a translational network of RNA-binding proteins controlled by HuR. *Nucleic Acids Res* 5: 3201-3216. PubMed: 23376935.
- Park S, Myszka DG, Yu M, Littler SJ, Laird-Offringa IA (2000) HuD RNA recognition motifs play distinct roles in the formation of a stable complex with AU-rich RNA. *Mol Cell Biol* 13: 4765-4772.
- Wang H, Li H, Shi H, Liu Y, Liu H et al. (2011) Preliminary crystallographic analysis of the RNA-binding domain of HuR and its poly(U)-binding properties. *Acta Crystallogr Sect Struct Biol Cryst Commun* 5: 546-550. PubMed: 21543858.
- Eberhardt W, Doller A, Akool el S, Pfeilschifter J (2007) Modulation of mRNA stability as a novel therapeutic approach. *Pharmacol Ther* 1: 56-73. PubMed: 17320967.
- Latorre E, Tebaldi T, Viero G, Spartà AM, Quattrone A et al. (2012) Downregulation of HuR as a new mechanism of doxorubicin resistance in breast cancer cells. *Mol Cancer* 11: 13. doi: 10.1186/1476-4598-11-13. PubMed: 22436134.
- Srikantan S, Gorospe M (2012) HuR function in disease. *Front Biosci* 17: 189-205. doi:10.2741/3921. PubMed: 22201738.
- Wang W, Furneaux H, Cheng H, Caldwell MC, Hutter D et al. (2000) HuR regulates p21 mRNA stabilization by UV light. *Mol Cell Biol* 3: 760-769. PubMed: 10629032.
- Abdelmohsen K, Kuwano Y, Kim HH, Gorospe M (2008) Posttranscriptional gene regulation by RNA-binding proteins during oxidative stress: implications for cellular senescence. *Biol Chem* 3: 243-255. PubMed: 18177264.

12. Sakai K, Kitagawa Y, Hirose G (1999) Binding of neuronal ELAV-like proteins to the uridine-rich sequence in the 3'-untranslated region of tumor necrosis factor-alpha messenger RNA. *FEBS Lett* 1: 157-162. PubMed: 10100634.
13. Rajasingh J, Bord E, Luedemann C, Asai J, Hamada H et al. (2006) IL-10-induced TNF-alpha mRNA destabilization is mediated via IL-10 suppression of p38 MAP kinase activation and inhibition of HuR expression. *FASEB J* 12: 2112-2114. PubMed: 16935932.
14. Kontoyannis D, Pasparakis M, Pizarro TT, Cominelli F, Kollias G (1999) Impaired on/off regulation of TNF biosynthesis in mice lacking TNF AU-rich elements: implications for joint and gut-associated immunopathologies. *Immunity* 3: 387-398. PubMed: 10204494.
15. Dean JL, Wait R, Mahtani KR, Sully G, Clark AR et al. (2001) The 3' untranslated region of tumor necrosis factor alpha mRNA is a target of the mRNA-stabilizing factor HuR. *Mol Cell Biol* 3: 721-730. PubMed: 11154260.
16. Tiedje C, Ronkina N, Tehrani M, Dharnija S, Laass K et al. (2012) The p38/MK2-driven exchange between tristetraprolin and HuR regulates AU-rich element-dependent translation. *PLOS Genet* 9:e1002977. PubMed: 23028373.
17. Eglén RM, Reisine T, Roby P, Rouleau N, Illy C et al. (2008) The use of AlphaScreen technology in HTS: current status. *Curr Chem Genomics* 1: 2-10. doi:10.2174/1875397300801010002. PubMed: 20161822.
18. Zhang JH, Chung TD, Oldenburg KR (1999) A Simple Statistical Parameter for Use in Evaluation and Validation of High Throughput Screening Assays. *J Biomol Screen* 2: 67-73.
19. Kim YU, Rus HG, Fisher SN, Pitha PM, Shin ML (1996) Binding of a protein to an AU-rich domain of tumour necrosis factor alpha mRNA as a 35 kDa complex and its regulation in primary rat astrocytes. *Biochem J* 2: 455-460.
20. Meisner NC, Hacker Müller J, Uhl V, Aszódi A, Jaritz M et al. (2004) mRNA openers and closers: modulating AU-rich element-controlled mRNA stability by a molecular switch in mRNA secondary structure. *ChemBiochem* 10: 1432-1447. PubMed: 15457527.
21. Fialcowitz-White EJ, Brewer BY, Ballin JD, Willis CD, Toth EA et al. (2007) Specific protein domains mediate cooperative assembly of HuR oligomers on AU-rich mRNA-destabilizing sequences. *J Biol Chem* 29: 20948-20959. PubMed: 17517897.
22. Chen YL, Huang YL, Lin NY, Chen HC, Chiu WC et al. (2006) Differential regulation of ARE-mediated TNFalpha and IL-1beta mRNA stability by lipopolysaccharide in RAW264.7 cells. *Biochem Biophys Res Commun* 1: 160-168. PubMed: 16759646.
23. Basu A, Datta D, Zurakowski D, Pal S (2010) Altered VEGF mRNA stability following treatments with immunosuppressive agents: implications for cancer development. *J Biol Chem* 285: 25196-25202. doi:10.1074/jbc.M110.119446. PubMed: 20554520.
24. Viiri J, Amadio M, Marchesi N, Hyttinen JMT, Kivinen N et al. (2013) Autophagy activation clears ELAV1/HuR-mediated accumulation of SQSTM1/p62 during proteasomal inhibition in human retinal pigment epithelial cells. *PLOS ONE*. doi:10.1371/journal.pone.0069563.
25. Chae MJ, Sung HY, Kim EH, Lee M, Kwak H et al. (2009) Chemical inhibitors destabilize HuR binding to the AU-rich element of TNF-alpha mRNA. *Exp Mol Med* 11: 824-831. PubMed: 19949288.
26. Meisner NC, Hintersteiner M, Mueller K, Bauer R, Seifert JM et al. (2007) Identification and mechanistic characterization of low-molecular-weight inhibitors for HuR. *Nat Chem Biol* 8: 508-515.
27. Tracey D, Klareskog L, Sasso EH, Salfeld JG, Tak PP (2008) Tumor necrosis factor antagonist mechanisms of action: a comprehensive review. *Pharmacol Ther* 2: 244-279. PubMed: 18155297.
28. Brennan CM, Steitz JA (2001) HuR and mRNA stability. *Cell Mol Life Sci* 2: 266-277. PubMed: 11289308.
29. Ross J (1996) Control of messenger RNA stability in higher eukaryotes. *Trends Genet* 5: 171-175. PubMed: 8984731.
30. Alberts DS, Griffith KS, Goodman GE, Herman TS, Murray E (1980) Phase I clinical trial of mitoxantrone: a new anthracenedione anticancer drug. *Cancer Chemother Pharmacol* 5(1): 11-15. doi:10.1007/BF00578556. PubMed: 7460190.
31. Kapuscinski J, Darzynkiewicz Z, Traganos F, Melamed MR (1981) Interactions of a new antitumor agent, 1,4-dihydroxy-5,8-bis[[2-(2-hydroxyethyl)amino]-ethyl]amino]-9,10-anthracenedione, with nucleic acids. *Biochem Pharmacol* 30(3): 231-240. doi: 10.1016/0006-2952(81)90083-6. PubMed: 7225141.
32. Edan G, Morrissey S, Le Page E (2004) Rationale for the use of mitoxantrone in multiple sclerosis. *J Neurol Sci*, 223(1): 35-39. doi: 10.1016/j.jns.2004.04.017. PubMed: 15261558.
33. Kapuscinski J, Darzynkiewicz Z (1986) Relationship between the pharmacological activity of antitumor drugs Ametantrone and mitoxantrone (Novatrone) and their ability to condense nucleic acids. *Proc Natl Acad Sci U S A* 83(17): 6302-6306. doi:10.1073/pnas.83.17.6302. PubMed: 3462696.
34. Zheng S, Chen Y, Donahue CP, Wolfe MS, Varani G (2009) Structural basis for stabilization of the tau pre-mRNA splicing regulatory element by novantrone (mitoxantrone). *Chem Biol*. 16(5):557-66